

DESY 01-098
HUPD-0107
TU-627

Revisiting $W\gamma$ production at RHIC

H. Kawamura

*Theory Group, DESY
Platanenallee 6 D 15738 Zeuthen, GERMANY*

Y. Kiyo

*Dept. of Physics, Tohoku University
Sendai 980-8578, JAPAN*

J. Kodaira and K. Morii

*Dept. of Physics, Hiroshima University
Higashi-Hiroshima 739-8526, JAPAN*

Abstract

We discuss $W\gamma$ production in polarized pp collisions at RHIC energy. We point out that the RHIC collider has two advantages over other hadron colliders to measure the characteristic feature of $W\gamma$ production: (1) the RHIC energy is not so high and (2) the polarized beams are available. We calculate the tree level cross section for $W\gamma$ production using a generic spin basis for W and discuss both the angular dependence and spin correlation.

1 Introduction

Radiative weak boson production in hadronic collisions has been extensively discussed for testing the electroweak structure of the standard model. Especially, the $W\gamma$ production has been the subject of much theoretical interests since this process contains the gauge boson trilinear coupling and develops the so-called radiation zero (RAZ) [1]. The phenomena RAZ is a typical example which is sensitive to the structure of electroweak interaction.

After the discovery of RAZ, the tree level [2] and higher order [3] analyses were done some years ago. Since the RAZ occurs only at the tree level of the fundamental process, the convolution of the partonic cross section with the parton distribution functions (PDFs) and the higher order QCD corrections to the fundamental process might give important effects and it is possible that RAZ is completely smeared out in the physical hadronic cross sections. There have been many efforts to calculate higher order corrections [4, 5, 6] in the standard model and phenomenological analyses [7] to utilize this process to test the standard model and/or find a signal from the model beyond the standard model [8].

Due to the $V - A$ structure of the W boson interaction, only the initial quarks which have definite helicities can participate in the process. Therefore an experiment with the polarized beams will be more efficient to study this process [9, 10].

Many works so far assumed rather high energy collisions. However, a realistic experiment with the polarized beams became available as the RHIC Spin Project whose center of mass energy is around $\sqrt{s} \sim 500$ GeV. In this article, we reanalyze the radiative weak boson production process at the RHIC energy. We argue that the experiment in the RHIC energy region will be very efficient to study this process if sufficient luminosity is achieved. From the experimental point of view, the detection of this process might not be so easy. We must be sure that the W boson is produced. The easiest signal would be the measurement of the momentum and angular distribution of the decay product, *e.g.* lepton, from W boson. This process, the weak boson production followed by its decay, is, in principle, a very complicated one. However, the narrow width approximation for the weak boson makes the situation very simple. We can discuss the production process and decay process separately. In the decay process, it is known that the distributions of decay products strongly depend on the direction of the spin of the produced W boson. So, it will be very interesting to know the cross section for the polarized W boson production. In this article, we present the polarized

W boson production in a “generic” spin basis according to ref. [11]. Although the authors in ref. [2] have already presented the contributions to the cross section from various spin configurations, the decomposition of the cross section in this article is new and will be more useful from the realistic point of view. One can expect that the “beamline basis” proposed in ref. [11] will be the most optimal spin basis here since the speed of the produced W would be small at the RHIC energy. We are mainly interested in the $W\gamma$ production process, however, we present the results also for the $Z\gamma$ production process.

Although the analyses in this article are based on the tree level calculations, we will give a discussion on the higher order QCD corrections which might be unimportant in the RHIC energy regime.

This paper is organized as follows. In Section 2, we give the tree level cross section for the polarized W and Z boson production in arbitrary spin basis. In Section 3, we calculate the hadronic cross section by convoluting the parton level cross section with the PDFs. Section 4 is devoted to a discussion on the results obtained in Section 3. Finally we give a summary in Section 5.

2 Polarized W^\pm and Z production

We discuss, in this section, the polarized weak boson production at the parton level. We demonstrate that the produced weak boson is predominantly polarized in the direction of the beam when its speed is not so large.

The tree level amplitude for the process,

$$q_1(q) + \bar{q}_2(\bar{q}) \rightarrow V(V) + \gamma(k) ,$$

where $V = W^\pm$ or Z , reads in the Feynman gauge,

$$\begin{aligned} M_{\lambda\lambda'}^{W^\pm} &= -\delta_{i_1 i_2} e^2 g_L^W \bar{v}(\bar{q}) \left[Q_1(\gamma_L)_\mu \frac{\not{q} - \not{k}}{u} \gamma_\nu + Q_2 \gamma_\nu \frac{\not{q} - \not{V}}{t} (\gamma_L)_\mu \right. \\ &+ \left. \frac{Q_2 - Q_1}{s - M_W^2} (\gamma_L)^\rho \{ (V - k)_\rho g_{\mu\nu} - (V + P)_\nu g_{\rho\mu} + (k + P)_\mu g_{\rho\nu} \} \right] u(q) \\ &\quad \times \epsilon_\lambda^{\mu*}(V) \epsilon_{\lambda'}^{\nu*}(k) . \end{aligned} \tag{1}$$

$$\begin{aligned} M_{\lambda\lambda'}^Z &= -\delta_{i_1 i_2} e^2 \sum_{\tau=L,R} g_\tau^Z \bar{v}(\bar{q}) \left[Q_1(\gamma_\tau)_\mu \frac{\not{q} - \not{k}}{u} \gamma_\nu + Q_2 \gamma_\nu \frac{\not{q} - \not{V}}{t} (\gamma_\tau)_\mu \right] u(q) \\ &\quad \times \epsilon_\lambda^{\mu*}(V) \epsilon_{\lambda'}^{\nu*}(k) . \end{aligned} \tag{2}$$

Here, $\delta_{i_1 i_2}$ is the color indices for the incoming quarks, $e(> 0)$ is the electromagnetic coupling constant and Q_i is the electric charge of quark q_i . For the Z boson production, $Q_1 = Q_2$. We define $P = q + \bar{q}$, $(\gamma_{L/R})_\mu = \gamma_\mu \frac{1 \mp \gamma_5}{2}$ and M_W is the W boson mass. $\epsilon_\lambda^{\mu*}(V)$ ($\epsilon_{\lambda'}^{\nu*}(k)$) is the W or Z (photon) polarization vector with spin index λ (λ'). The weak boson-to-quark couplings g_L^W , $g_{L/R}^Z$ are given by,

$$g_L^W = \frac{V_{q_1 q_2}}{\sqrt{2} \sin \theta_W} \quad , \quad g_L^Z = \frac{T_3^i}{\sin \theta_W \cos \theta_W} - Q_i \tan \theta_W \quad , \quad g_R^Z = -Q_i \tan \theta_W \quad ,$$

where θ_W is the Weinberg angle, $V_{q_1 q_2}$ is the Cabibbo-Kobayashi-Maskawa matrix and T_3^i is the third component of weak isospin of q_i . The parton level invariants s, t, u are defined as usual,

$$s = (q + \bar{q})^2 \quad , \quad t = (q - V)^2 \quad , \quad u = (q - k)^2 \quad .$$

Using the equation of motion for external particles, both eqs.(1) and (2) can be compactly expressed as,

$$M_{\lambda\lambda'}^V = -\delta_{i_1 i_2} e^2 \sum_{\tau=L,R} g_\tau^V \frac{Q_1 t + Q_2 u}{t + u} \\ \times \bar{v}(\bar{q}) \left[2 \left(\frac{q_\mu}{t} - \frac{\bar{q}_\mu}{u} \right) \gamma_\nu - \frac{2}{t} (V_\nu \gamma_\mu - g_{\mu\nu} \not{V}) - \frac{t+u}{tu} \not{V} \gamma_\mu \gamma_\nu \right] \omega_\tau u(q) \epsilon_\lambda^{\mu*}(V) \epsilon_{\lambda'}^{\nu*}(k) \quad ,$$

with $\omega_{L/R} = \frac{1 \mp \gamma_5}{2}$. The particular combination of charge and kinematical variables,

$$\frac{Q_1 t + Q_2 u}{t + u} \quad ,$$

leads to the phenomena called Radiation Zeros for the W production.

Assuming that we will measure only polarized V boson, we sum up the photon polarization in the square of amplitude.

$$\frac{d\sigma^\lambda}{dt du} = \frac{1}{16\pi s^2} \frac{1}{N_c^2} \sum_{\text{color}, \lambda'} |M_{\lambda\lambda'}^V|^2 \delta(s + t + u - M_V^2) \quad . \quad (3)$$

N_c is the number of colors and M_V denotes the mass of W or Z . In the zero momentum frame (ZMF), this expression becomes,

$$\frac{d\sigma^\lambda}{d \cos \theta} = \frac{1}{32\pi s} \left(1 - \frac{M_V^2}{s} \right) \frac{1}{N_c^2} \sum_{\text{color}, \lambda'} |M_{\lambda\lambda'}^V|^2 \\ \equiv \frac{e^4 (g_{L/R}^V)^2}{32 N_c \pi s} \left(1 - \frac{M_V^2}{s} \right) \left(\frac{Q_1 t + Q_2 u}{t + u} \right)^2 \frac{1}{tu} \mathcal{S}_{L/R}^\lambda \quad , \quad (4)$$

where the angle θ is the scattering angle of the V boson with respect to the quark q_1 direction.

$$t = -\frac{s - M_V^2}{2} (1 - \cos \theta) \quad , \quad u = -\frac{s - M_V^2}{2} (1 + \cos \theta) .$$

In this paper, we use the spinor helicity method with the generic spin basis proposed in ref. [11]. According to ref. [12], we introduce the spin vector S such that $S^2 = -1$ and $V \cdot S = 0$. The V boson has spin projection $\epsilon_\lambda^{\mu*}(V)$ ($\lambda = +, 0, -$) with respect to the spatial part of S in the rest frame of V . These three polarization vectors can be written in terms of massless spinors with momenta, $V_1 = (V + M_V S)/2$, $V_2 = (V - M_V S)/2$ as,

$$\begin{aligned} \epsilon_\pm^{\mu*}(V) &= \frac{\langle V_1 \pm |\gamma^\mu| V_2 \pm \rangle}{\sqrt{2} M_V} , \\ \epsilon_0^{\mu*}(V) &= \frac{\langle V_1 + |\gamma^\mu| V_1 + \rangle - \langle V_2 + |\gamma^\mu| V_2 + \rangle}{2 M_V} = \frac{V_1^\mu - V_2^\mu}{M_V} . \end{aligned}$$

The spin vector for V is parameterized by the angle ξ in its rest frame measured from the γ direction as given in Fig.1. Choosing the z-axis to be the direction of V momentum in the ZMF, the momenta of particles and the vector V_i turn out to be,

$$\begin{aligned} q &= \frac{\sqrt{s}}{2} (1, \sin \theta, 0, \cos \theta) \quad , \quad \bar{q} = \frac{\sqrt{s}}{2} (1, -\sin \theta, 0, -\cos \theta) , \\ V &= M_V \gamma (1, 0, 0, \beta) \quad , \quad k = M_V \gamma \beta (1, 0, 0, 1) , \\ V_1 &= \frac{M_V}{2} (\gamma(1 - \beta \cos \xi), -\sin \xi, 0, \gamma(\beta - \cos \xi)) , \\ V_2 &= \frac{M_V}{2} (\gamma(1 + \beta \cos \xi), \sin \xi, 0, \gamma(\beta + \cos \xi)) , \end{aligned} \tag{5}$$

where β is the speed of V boson,

$$\beta = \frac{s - M_V^2}{s + M_V^2} ,$$

and $\gamma = (1 - \beta^2)^{-1/2}$ is the usual relativistic factor.

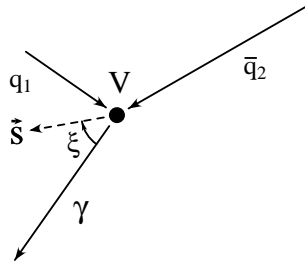


Figure 1: \vec{s} is the spin vector associated with V in its rest frame.

After straightforward manipulations, we obtain,

$$\mathcal{S}_{L/R}^0 = 2 \left[t^2 + u^2 + 2M_V^2 s - 4(a^2 + b^2) \right] , \quad (6)$$

$$\mathcal{S}_{L/R}^\pm = t^2 + u^2 + 2M_V^2 s + 4(a^2 + b^2) (\pm/\mp) 4 \{ (s+u)a - (s+t)b \} , \quad (7)$$

where we have defined,

$$a = q \cdot (V_1 - V_2) , \quad b = \bar{q} \cdot (V_1 - V_2) .$$

Summing over the three possible spins of V , we recover the usual expression from eqs.(6,7),

$$\sum_\lambda \mathcal{S}_{L/R}^\lambda = 4 \left[t^2 + u^2 + 2M_V^2 s \right] ,$$

for the unpolarized cross section which is independent of the spin axis angle ξ , as it must be.

In the case of the hadronic reaction, we must finally convolute the partonic cross section eq.(3) with the PDFs. In such a case, the following two spin bases are sensible. Let us consider the W^\pm production for definiteness. In this case, only the left-hand coupling is present ($\tau = L$). The first is the usual helicity basis ($\xi = \pi$). Inserting $\xi = \pi$ to eq.(5), eqs.(6,7) become,

$$\mathcal{S}_L^0 = 4M_W^2 s \sin^2 \theta \quad , \quad \mathcal{S}_L^\pm = 2M_W^2 s \frac{1 + \beta^2}{1 - \beta^2} (1 \mp \cos \theta)^2 . \quad (8)$$

From these expressions, one can see that all spin configurations equally contribute to the cross section for finite β .

The second is the so-called beamline basis [11], which is defined by,

$$\cos \xi = \frac{\cos \theta + \beta}{1 + \beta \cos \theta} \quad , \quad \sin \xi = \frac{\sqrt{1 - \beta^2} \sin \theta}{1 + \beta \cos \theta} . \quad (9)$$

In this basis, the spin axis for W is the direction of one of the beams \bar{q}_2 . Inserting again eq.(9) to eq.(5), we obtain in this case from eqs.(6,7),

$$\begin{aligned} \mathcal{S}_L^0 &= 8M_W^2 s \frac{1}{(1 + \beta \cos \theta)^2} \beta^2 \sin^2 \theta , \\ \mathcal{S}_L^- &= 4M_W^2 s \frac{1}{(1 + \beta \cos \theta)^2} \frac{\beta^4}{1 - \beta^2} \sin^4 \theta , \\ \mathcal{S}_L^+ &= 4M_W^2 s \frac{1}{(1 + \beta \cos \theta)^2} \frac{1}{1 - \beta^2} \left\{ (1 - \beta^2)^2 + (1 + \beta \cos \theta)^4 \right\} . \end{aligned} \quad (10)$$

From these results, we can see that the the cross sections with the polarization, 0 and $-$ are suppressed when the speed β of W is small. This is consistent with the following observation. Due to the $V - A$ structure of the weak interaction, the spins of the initial quarks are aligned to the direction of \vec{q}_2 momentum. Therefore near the threshold, only the $+$ component survives.

We present in Fig.2 (Fig.3) the differential cross section for $W\gamma$ ($Z\gamma$) production at partonic level in the beamline and helicity bases. For the Z production, we plot only the $q_L\bar{q}_R$ case. We take the center-of-mass energy to be $\sqrt{s} = 100$ GeV which would be a typical energy scale of the partonic sub-process in the RHIC energy regime.

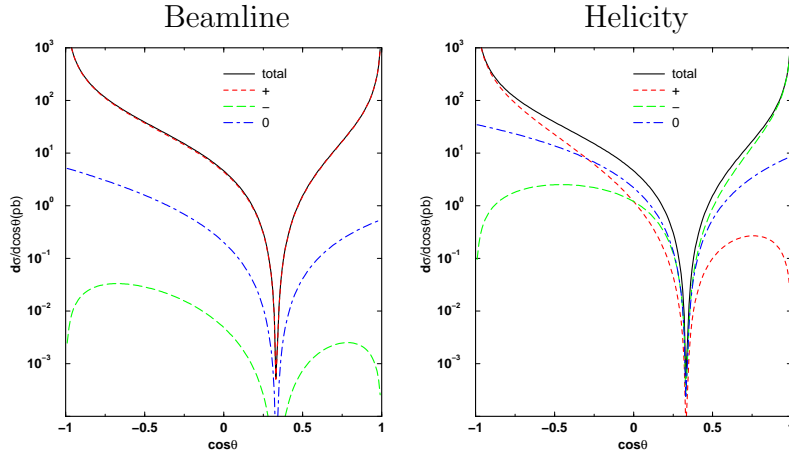


Figure 2: $W\gamma$ production in the partonic ZMF.

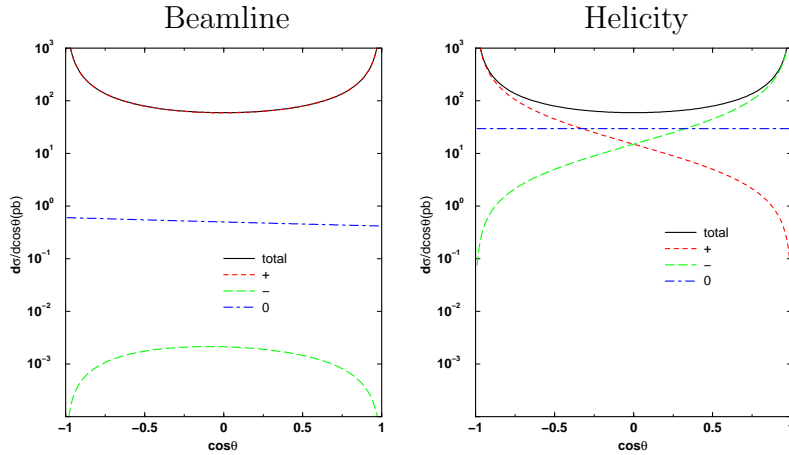


Figure 3: $Z\gamma$ production in the partonic ZMF.

Except for the fermion masses, which we neglect, all input masses and coupling constants used in the numerical computations are the central values as reported in the 2000 Review of Particle Physics [13].

For both W and Z productions, only one component, namely $+$ component, dominates the cross section and contributions from other spin configurations are less than several percents in the beamline basis as expected since the β is small, $\beta \sim 0.2$. This means that the direction of the spin of produced weak boson at RHIC is almost the beam direction. On the other hand, the helicity basis is a poor basis in the sense that all components of spin contribute equally to the cross section as seen in Figs.2. and 3. For the Z production, the helicity state of the quarks, $q_R\bar{q}_L$ also contributes. In this case, the polarization indices \pm in eqs.(8,10) should be exchanged and the interpretation of the results is the same as for the W production case.

3 Hadronic cross section

We present the hadronic cross section by convoluting the previous parton cross sections with the PDFs. In this section, we shall limit ourselves to the $W^+\gamma$ production and calculate the angular distribution of the produced γ as shown in Fig.4 simply due to

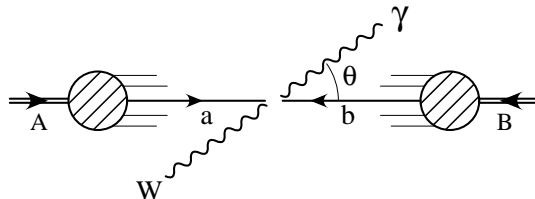


Figure 4: The process $pp \rightarrow W\gamma X$.

the easier kinematics. Furthermore we consider the spin-summed cross section because we already know that the spin of the produced W is in the beam direction.

At first, we summarize the polarized quark distribution function in the polarized proton and give qualitative arguments on the results expected.

3.1 Parton distribution functions

We consider only the contributions from u and d quarks since the Cabibbo angle is $\sin^2\theta_C \sim 0.05$ and the number of s and c quarks is expected to be small. We

use the notation $q_{\pm}(x, Q^2)$ for the quark distribution in a polarized proton with the momentum fraction x at the scale Q^2 , where $+(-)$ refers to a quark with helicity parallel (antiparallel) to the parent proton's helicity. These quark densities roughly satisfy,

$$u_+(x, Q^2) \gg d_-(x, Q^2) \sim u_-(x, Q^2) \gg d_+(x, Q^2) \gg \bar{u}_{+,-}(x, Q^2) \sim \bar{d}_{+,-}(x, Q^2) , \quad (11)$$

for almost all x at the relevant scale $Q^2 \simeq M_W^2$.

The V-A structure of interaction picks up only quarks which have definite helicities. Therefore the partonic contents which contribute to the hadronic cross section $d\sigma_{h_A h_B}$ where $h_A, h_B = \pm$ denote the proton's helicities, are the followings.

$$\begin{aligned} d\sigma_{++} &: u_-(x_A, Q^2)\bar{d}_+(x_B, Q^2) + u \leftrightarrow \bar{d} , \\ d\sigma_{+-} &: u_-(x_A, Q^2)\bar{d}_-(x_B, Q^2) + \bar{d}_+(x_A, Q^2)u_+(x_B, Q^2) , \\ d\sigma_{-+} &: u_+(x_A, Q^2)\bar{d}_+(x_B, Q^2) + \bar{d}_-(x_A, Q^2)u_-(x_B, Q^2) , \\ d\sigma_{--} &: u_+(x_A, Q^2)\bar{d}_-(x_B, Q^2) + u \leftrightarrow \bar{d} . \end{aligned} \quad (12)$$

From these expressions and eq.(11), we expect that: (1) the size of the cross section is $d\sigma_{--} > d\sigma_{+-} = d\sigma_{-+} > d\sigma_{++}$, (2) the angular distributions become asymmetric for $d\sigma_{+-}$ and $d\sigma_{-+}$ due to the RAZ of their sub-processes.

3.2 Covolution

For the reaction,

$$p(P_A) + p(P_B) \rightarrow W^+(q) + \gamma(k) + X ,$$

the differential cross section for the photon can be derived from the expression,

$$s \frac{d\sigma_{h_A h_B}}{dt du} = \int dx_A dx_B f_{h_A}^i(x_A, Q^2) f_{h_B}^j(x_B, Q^2) \hat{s} \frac{d\hat{\sigma}_{ij}}{d\hat{t} d\hat{u}} , \quad (13)$$

where f_{h_A, h_B}^i stands for one of the quark distributions, eq.(11). Here $d\hat{\sigma}_{ij}$ denote the partonic cross sections eq.(3) where $i(j)$ corresponds to a parton from proton A (B). The Mandelstam variable in the hadron system are defined by,

$$s = (P_A + P_B)^2 , \quad t = (P_A - k)^2 , \quad u = (P_B - k)^2 .$$

Therefore the partonic variables are,

$$\hat{s} = x_A x_B s , \quad \hat{t} = x_A t , \quad \hat{u} = x_B u .$$

From eqs.(13) and (3), the angular distribution of photon in proton's ZMF becomes,

$$\frac{d\sigma_{h_A h_B}}{d \cos \theta_\gamma} = \frac{1}{8\pi s} \int k^0 dk^0 \frac{dx_A}{x_A} \frac{dx_B}{x_B} f_{h_A}^i(x_A, Q^2) f_{h_B}^j(x_B, Q^2) \quad (14)$$

$$\times \frac{1}{N_c^2} \sum_{\text{color}, \lambda, \lambda'} |M_{\lambda\lambda'}^W|^2 \delta(\hat{s} + \hat{t} + \hat{u} - M_W^2),$$

where k^0 is the energy of photon and it is understood that i, j take appropriate partons according to eq.(12).

We plot the hadronic cross section in Fig.5 at $\sqrt{s} = 500\text{GeV}$ using the parameterization in ref. [14] with $Q^2 = M_W^2$ for the (quark) parton densities. To avoid the soft photon singularity or take into account the experimental situation, we have chosen the

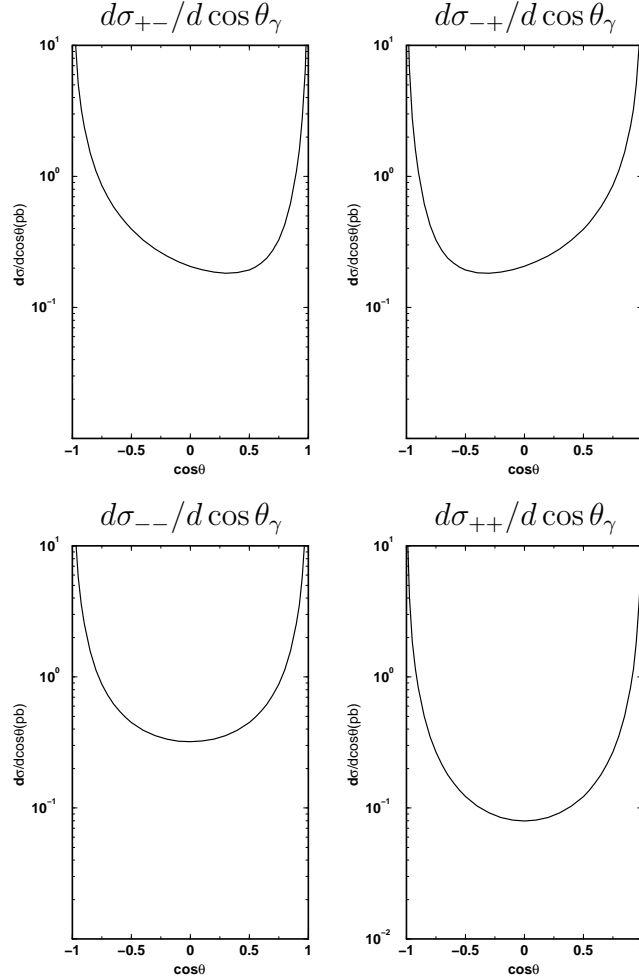


Figure 5: The photon distribution in the laboratory frame at $\sqrt{s} = 500 \text{ GeV}$.

minimum cut-off energy for the photon to be 5 GeV. One can see a rather clear signal from RAZ in the cross section when the initial proton's helicities are parallel each other. This is because the helicity distributions of quarks depend on the spin of the parent protons. Note that if the proton contains the equal parton densities of both helicity states as for the unpolarized case, the convolution completely smears out the RAZ.

We define also an asymmetry by,

$$A = \frac{d\sigma_{-+}/d\cos\theta_\gamma - d\sigma_{+-}/d\cos\theta_\gamma}{d\sigma_{-+}/d\cos\theta_\gamma + d\sigma_{+-}/d\cos\theta_\gamma},$$

and plot it in Fig.6. This asymmetry amounts to $\sim 40\%$.

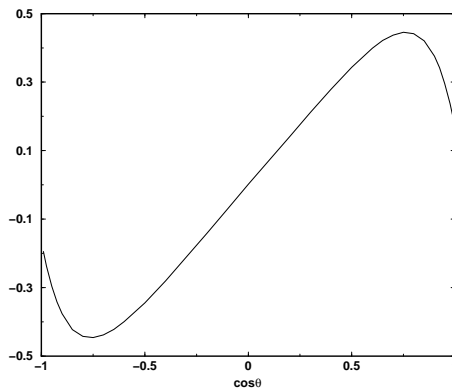


Figure 6: Asymmetry with respect to $\cos\theta_\gamma$.

4 Discussion

The RAZ is a prominent feature of the electroweak standard model. However, it occurs only at the partonic tree level. Therefore in the experimental measurements, we must seriously consider the two effects which possibly wash out the RAZ: (1) the effects from the PDF (2) radiative corrections. In this section, we discuss why the experiment at RHIC energy with polarized beams is appropriate for studying the radiative weak boson productions.

Let us first consider the effects coming from the convolution of the partonic cross section with the PDFs. Due to the $V - A$ structure of the W boson interaction, the partonic process strongly depends on the helicity states of initial quarks. However if the proton contains the equal parton densities of both helicity states as for the unpolarized

case, the convolution smears out the RAZ. In the case of the polarized beams, it is known that the helicity distribution of partons strongly depend on the spin of parent hadrons. Therefore, the RAZ will not be completely smeared out in the polarized collisions as shown in Fig.5. Actually, this was the main idea of ref. [9]. How about is the energy dependence of this smearing effect? It is easily understood that the dip will be more smeared as the energy becomes higher. It is because the small x partons start to participate in the process at higher energy and those sea partons carry less information of the parent proton's spin. Namely the contribution from the small x partons is expected to be the same both for the polarized and unpolarized protons. To verify this feature, we calculate the cross section at $\sqrt{s} = 2000$ GeV and plot it in

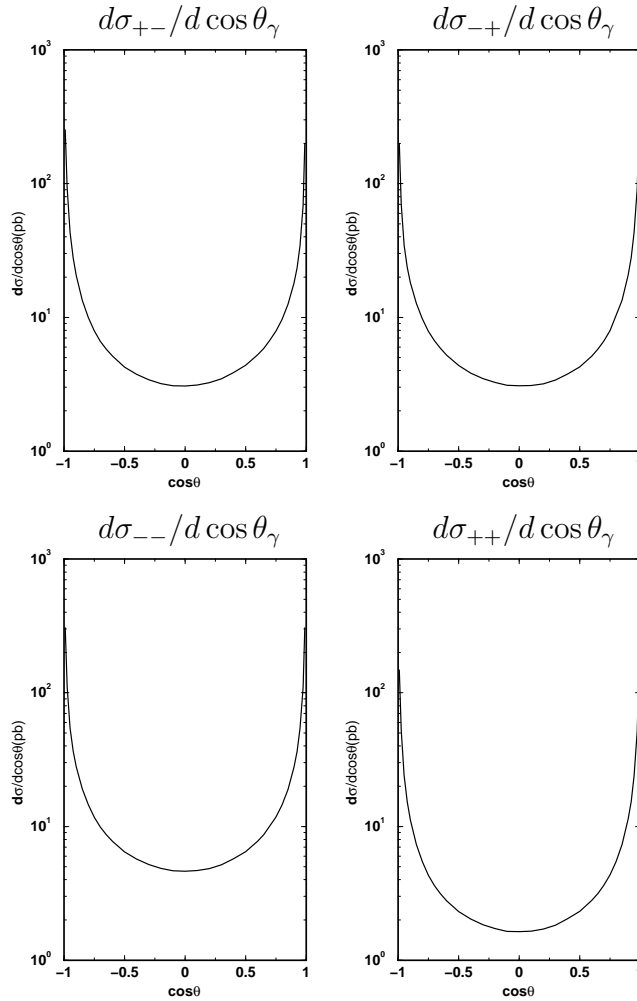


Figure 7: The photon distribution in the laboratory frame at $\sqrt{s} = 2000$ GeV.

Fig.7. One can see that the angular distribution become symmetric for all proton's spin configurations and the RAZ is completely smeared out.

Secondly we discuss the effects of radiative QCD corrections. In general, since the tree level cross section develops zero, the radiative corrections are very important. The QCD corrections to these process were calculated in refs.[4, 5] and detailed numerical analyses have been done. The radiative corrections can be classified into three effects: (1) virtual corrections and soft gluon emissions (2) hard gluon emissions (3) initial gluon process $q_1 g \rightarrow V \gamma q_2$ and $g \bar{q}_2 \rightarrow V \gamma \bar{q}_1$. Among these effects, the first one leaves the RAZ intact. Its main effect is a constant K factor. The second and third effects, on the other hand, will completely wash out the RAZ phenomena. These effects, however, have been known to be important at large energies [4]. It is, therefore, expected that in the RHIC energy region, it is sufficient to include only the first effect. As stated above, this effect will not change the shape of the cross section from the tree level one. Therefore the results of the previous section remain the same qualitatively except for some multiplicative enhancement. In particular, the asymmetry, Fig.6, remains the same.

5 Summary

We have studied the radiative weak boson production at RHIC energy. We have pointed out that the experiments in the RHIC energy region will be very efficient to study this process. Although the analyses in this article were based on the tree level calculations, we argued that the higher order QCD corrections will not smear out the dips from RAZ at intermediate energies. Furthermore the polarized beams at RHIC develop these dips. In the case of pp collision, the unpolarized experiment leads to only the symmetric angular distributions for the photon. We can hope that the phenomena, RAZ will survive many possible smearing effects at the RHIC polarized experiments.

Acknowledgment

The work of J.K. was supported in part by the Monbu-kagaku-sho Grant-in-Aid for Scientific Research No. C-13640289. Y.K. was supported by the Japan Society for the Promotion of Science.

References

- [1] R.W. Brown and K.O. Mikaelian, *Phys. Rev.* **D19** (1979) 922.
R.W. Brown, K.O. Mikaelian and D. Shaddev, *Phys. Rev.* **D20** (1979) 1164.
K.O. Mikaelian, M. A. Samuel and D. Shaddev, *Phys. Rev. Lett.* **43** (1979) 746.
- [2] M. Hellmund and G. Ranft, *Z. Phys.* **C12** (1982) 333.
- [3] V. Berger, T. Han, D. Zeppenfeld and J. Ohnemus, *Phys. Rev.* **D41** (1990) 2782.
- [4] J. Smith, W. L. van Neerven and J. A. M. Vermaseren, *Z. Phys.* **C30** (1986) 621.
J. Smith, D. Thomas and W. L. van Neerven, *Z. Phys.* **C44** (1989) 267.
S. Mendoza, J. Smith and W. L. van Neerven, *Phys. Rev.* **D47** (1993) 3913.
- [5] J. Ohnemus, *Phys. Rev.* **D47** (1993) 940.
- [6] U. Baur, T. Han, N. Kauer, R. Sobey and D. Zeppenfeld, *Phys. Rev.* **D56** (1997) 140.
- [7] U. Baur, T. Han and J. Ohnemus, *Phys. Rev.* **D48** (1993) 5140; and references therein.
- [8] for a recent article, see D. de Florian and A. Signer, *Eur. Phys. J.* **C16** (2000) 105; and references therein.
- [9] M. Wiest, D. R. Stump, D. O. Carlson and C. -P. Yuan, *Phys. Rev.* **D52** (1995) 2724.
- [10] M. Han, W. -G. Ma, L. Han Y. Jiang, *J. Phys.* **G24** (1998) 551.
- [11] G. Mahlon and S. Parke, *Phys. Rev.* **D53** (1996) 4886; *Phys. Lett.* **B411** (1997) 173.
- [12] G. Mahlon and S. Parke, *Phys. Rev.* **D58** (1998) 054015.
- [13] D. E. Groom *et al*, *Eur. Phys. J.* **C15** (2000) 1.
- [14] A.D. Martin, W.J. Stirling and R.G. Roberts, *Phys. Rev.* **D50** (1994) 6734.
T. Gehrmann and W. J. Stirling, *Phys. Rev.* **D53** (1996) 6100.